Journal of Engineering, Project, and Production Management
2026, 16(7), 2025-342

A Hybrid Multi-Objective Optimization Framework for Crop Planting Planning under Digital Economy

Xiaohong Wang
Deputy Director, Center for Contemporary Marxist Economics Research, Zhengzhou Technology and Business University, 451400, China, E-mail: wang_xhong@outlook.com

Project Management
Received December 18, 2025; revised February 4, 2026; accepted July 12, 2026
Available online July 25, 2026

Abstract: With the deep integration of artificial intelligence and the digital economy in agriculture, traditional crop planting planning still suffers from slow convergence, limited optimization accuracy, and weak adaptability to ecological and market uncertainties. To address these challenges, this study proposes a multi-objective crop planting optimization model that integrates the Multi-Objective Grey Wolf Optimizer (MOGWO), the non-dominated sorting genetic algorithm II, and proximal policy optimization, enabling dynamic decision-making driven by multi-source data. Experimental results on two authoritative datasets showed that the model achieved Pareto frontier coverage above 90% and stable convergence within 500 iterations. Multi-scenario simulations indicated that peak annual net profit exceeded 1.8 million yuan, and annual carbon reduction potential generally exceeded 150 tons of CO_2, while computation time was maintained at approximately 4.8s per 100 iterations. Overall, the proposed model demonstrates strong robustness, ecological effectiveness, and computational efficiency, supporting intelligent agricultural decision-making under the digital economy framework.

Keywords: Digital economy; multi-objective optimization; MOGWO; crop planting planning; ecological benefits.

DOI 10.32738/JEPPM-2025-342

1. Introduction

Rapid population growth and urban–rural integration have intensified the dual challenges of food security and ecological conservation in modern agriculture. Climate change has limited arable land, and the environmental risks of fertilizer and pesticide overuse have revealed the shortcomings of traditional yield-oriented farming systems (Rahman et al., 2025). Meanwhile, the expansion of the digital economy driven by technologies such as the Internet of Things, artificial intelligence, and cloud computing has enabled precision management and low-carbon agricultural practices. Against this backdrop, balancing food security with ecological sustainability while improving system efficiency through digital technologies has become an urgent research focus, prompting growing interest in crop planting strategies that jointly optimize economic and ecological outcomes (Michels et al., 2024).

Chikkasiddaiah et al. (2023) developed a crop growth prediction system for water and nutrient management by modeling relationships among nutrient indices, electrical conductivity, and crop yield, thereby effectively increasing the proportion of high-quality production. Choudhury et al. (2024) proposed a fertilization planning framework that combines decision trees and logistic regression, achieving an 85.7% optimization rate for fertilizer ratios under economic-benefit constraints. Alhussan et al. (2024) integrated the Hydro Turbine Power Plant optimization algorithm with an autoregressive integrated moving average model to optimize potato planting ratios, attaining high predictive accuracy with a root mean square error of 0.0001. Guo et al. (2024) enhanced corn cultivation intelligence by incorporating You Only Look Once version 8 (YOLOv8) into the navigation of spraying robots, enabling precise route planning and yield improvement through accurate plant localization. Yadav et al. (2025) applied genetic algorithms to optimize parental selection in crop breeding, improving wheat genotype configuration and mitigating the negative impact of unfavorable genes on plant survival. Existing crop planting planning studies have mainly relied on single-objective or multi-objective optimization techniques. While effective for medium- to low-dimensional problems, these methods often suffer from slow convergence, susceptibility to local optima, and limited adaptability to complex ecological constraints in high-dimensional decision scenarios. In this context, the multi-objective grey wolf optimizer has attracted increasing attention due to its simple structure, few control parameters, and fast convergence (Hussien et al., 2024). Recent studies have applied the Multi-Objective Grey Wolf Optimizer (MOGWO) to surface–groundwater management (Torabi et al., 2024), reservoir zoning optimization (Bajelani et al., 2024), Pareto frontier approximation and scheduling (Qiu, 2024), wastewater collection and treatment (Mahmoodabadi et al., 2024), and intelligent system configuration (Wang and Zhou, 2025), demonstrating its strong search efficiency and solution stability across diverse application domains.

In summary, existing crop planting planning methods remain limited by slow convergence, suboptimal decision accuracy, and limited adaptability to dynamic environments, market fluctuations, and quantified ecological constraints, thereby restricting the joint achievement of yield robustness and ecological synergy in the digital economy. To overcome these limitations, this study proposes a multi-level synergistic optimization framework integrating MOGWO, Non-dominated Sorting Genetic Algorithm II (NSGA-II), and Proximal Policy Optimization (PPO). Moreover, MOGWO enables global exploration, NSGA-II ensures balanced maintenance of Pareto solutions, and PPO supports dynamic, risk-aware adaptation, collectively enhancing search efficiency, frontier quality, and robustness under uncertainty. Compared to existing single-heuristic or static multi-objective models, the proposed method achieves synergistic improvements in global search capability, Pareto frontier distribution equilibrium, and dynamic environmental adaptability. Furthermore, the study incorporates real-time market prices, climate-driven factors, and ecological constraints into the optimization process. This establishes a unified revenue-cost-ecology multi-objective modeling system that deeply integrates digital economic information with intelligent optimization algorithms. The main innovations of this study include a three-layer collaborative optimization framework of "global search-elite retention-dynamic strategy". This study introduces a reinforcement learning mechanism to describe the risk management process under price fluctuations and climate uncertainty. Moreover, this study systematically validates the model's comprehensive advantages in revenue robustness, emissions reduction, and computational efficiency using authoritative agricultural and meteorological datasets. These findings provide a scalable technical pathway for intelligent agricultural decision-making driven by the digital economy.

2. Methods and Materials

The proposed framework integrates MOGWO-based global search, NSGA-II–based elite refinement, and PPO-driven dynamic adaptation, incorporating real-time price and climate feedback, to jointly optimize economic returns, input costs, ecological emissions reduction, and output efficiency in crop planting planning.

2.1. MOGWO Algorithm and its Improved Optimization

Traditional single-objective or linear optimization methods are inadequate for such scenarios, underscoring the need for efficient, intelligent algorithms for high-dimensional search spaces (Sarkar et al., 2024; Sankareshwaran et al., 2023; Cai et al., 2023). Inspired by grey wolf social behavior, the multi-objective grey wolf optimizer achieves effective global exploration and local exploitation with a simple structure and fast convergence, making it well suited for complex multi-objective optimization problems (Sheikh et al., 2024; Bilal et al., 2023). The overall process of the MOGWO algorithm is shown in Fig. 1.

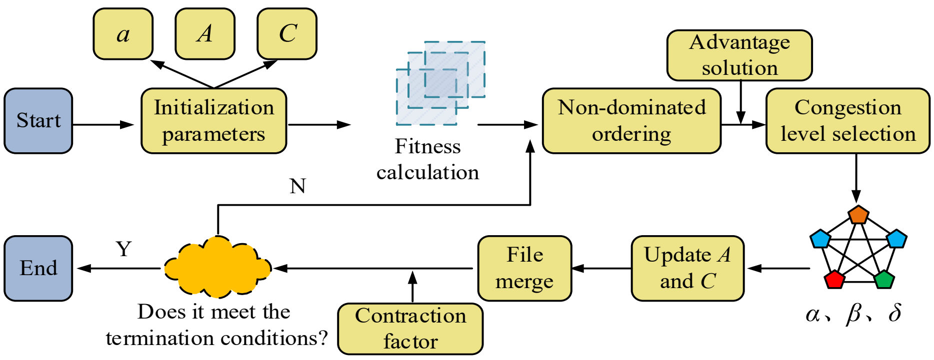

Fig. 1. The overall process of the MOGWO algorithm

In Fig. 1, the MOGWO solution begins by initializing the population with parameters a, A, and C. It calculates the fitness of individuals across multiple objectives and performs non-dominated sorting, storing superior solutions in an external archive. Current leading individuals α, β, and δ are selected based on crowding. The main loop then proceeds as follows: For each grey wolf, A and C are updated using random coefficients. Three candidate moves are computed by referencing the positions of α, β, and δ respectively, and their means are averaged to derive new positions. Out-of-bounds points are repaired within the feasible domain. The new solution is re-evaluated, and after merging with the archive, truncation is performed according to the principle of "non-domination priority, followed by crowding degree," to redefine α, β, and δ. The capture coefficient and contraction factor ϑ updates are expressed as shown in Eq. (1) (Heimstädt, 2023; Demilie, 2024; Zhang et al., 2024).

$$\begin{cases} A = 2\vartheta r_1 - \vartheta \\ C = 2r_2 \\ \vartheta(t) = 2 - 2\frac{t}{T} \end{cases} \tag{1}$$

In Eq. (1), r_1 and r_2 both represent independent uniform random variables. A and C denote the capture control vectors. $\vartheta(t)$ represents the contraction factor for the tth generation, which decreases linearly with the maximum generation number T to enhance late-stage development capability. Position updates are coordinated with the three leaders as shown in Eq. (2) (Liu, 2023; Ahila et al., 2024; Ghosh et al., 2023).

$$\begin{cases} D_\alpha = |C_1 \otimes X_\alpha - X(t)|, X_1 = X_\alpha - A_1 \otimes D_\alpha \\ D_\beta = |C_2 \otimes X_\beta - X(t)|, X_2 = X_\beta - A_2 \otimes D_\beta \\ D_\delta = |C_3 \otimes X_\delta - X(t)|, X_3 = X_\delta - A_3 \otimes D_\delta \\ X(t+1) = \frac{X_1+X_2+X_3}{3} \end{cases} \tag{2}$$

In Eq. (2), $X(t)$ denotes the current individual position vector. X_α, X_β, and X_δ represent the predicted positions of the three types of leader wolves. D_α, D_β, and D_δ denote the actual positions of the three types of leader wolves. $\otimes$ signifies the Hadamard multiplication by dimension. (A_k, C_k) indicates the generation of random numbers and ϑ respectively, according to the preceding equation, used for adaptive switching between exploration ($|A_k| > 1$) and exploitation ($|A_k| < 1$). However, baseline MOGWO exhibits biased Pareto set maintenance, which is alleviated by integrating NSGA-II for efficient non-dominated sorting and diversity control (Fig. 2) (Singh et al., 2025; Pitakaso et al., 2024; Yang et al., 2024).

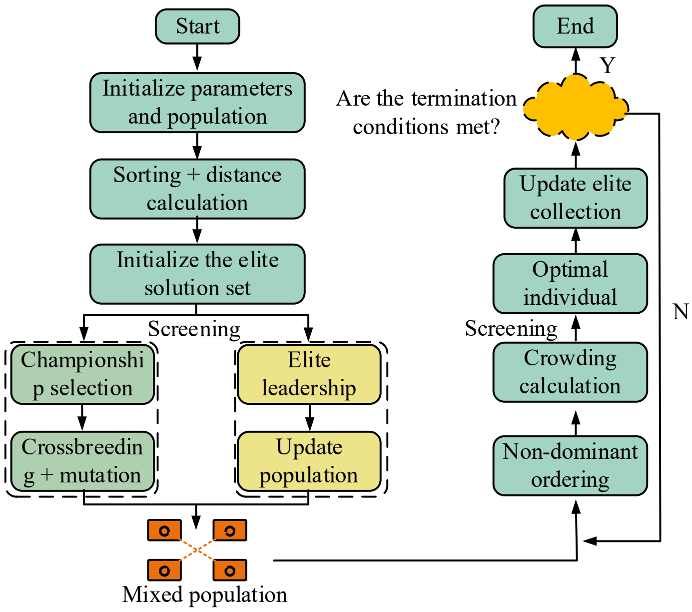

Fig. 2. The MOGWO-NSGA-II process

As illustrated in Fig. 2, the MOGWO-NSGA-II hybrid algorithm combines MOGWO-based leader-guided global search with NSGA-II–based elite archive management, selection, and genetic variation. Solutions generated by both mechanisms are merged and refined through non-dominated sorting and crowding-distance-based selection to maintain Pareto diversity until convergence, yielding the final optimal scheme. The tournament selection probability is defined in Eq. (3).

$$P_{sel}(i,j) \begin{cases} 1 & if\_i > j \\ \frac{1}{2} & if\_i = j \\ 0 & f\_i < j \end{cases} \tag{3}$$

In Eq. (3), i and j represent any two candidate individuals. When individual i outperforms j over $P_{sel}(i,j) = 1$, and if the two do not mutually dominate, i is selected with a 0.5 probability to ensure superior individuals are prioritized for inheritance. MOGWO-NSGA-II simulates binary crossover to generate offspring, as shown in Eq. (4).

$$X_k^{'} = \frac{1}{2}\left[(1+\beta_k)X_p + (1-\beta_k)X_q\right] \tag{4}$$

In Eq. (4), X_p and X_q both represent the parent generation solution vector. X_k' denotes the offspring solution. $X_k^{'}$ represents the real-valued encoding parameter for genetic recombination. The crowding distance update at this stage is given by Eq. (5).

$$CD_i^{new} = \sum_{m=1}^{M} \frac{f_m^{i+1} - f_m^{i-1}}{f_m^{\max} - f_m^{\min}} \tag{5}$$

In Eq. (5), CD_i^{new} denotes the crowding distance of the new generation individual i in the m dimension. Among them, a larger CD_i^{new} indicates that the solution resides in a sparse region, making it more likely to be retained to maintain the breadth and uniform distribution of the Pareto front. To further enhance the algorithm's adaptability in dynamic environments such as real-time price fluctuations and climate uncertainties, the study introduces PPO to build a reinforcement learning layer that collaborates with MOGWO-NSGA-II (Liang et al., 2024). During the coupling process of MOGWO-NSGA-PPO, the shear probability is calculated using the objective function as shown in Eq. (6).

$$L^{CLIP}(\theta) = E_t[min(r_t(\theta)\hat{A}_t, clip(r_t(\theta), 1-\varepsilon, 1+\varepsilon)\hat{A}_t)] \tag{6}$$

In Eq. (6), $r_t(\theta)$ denotes the probability ratio between the current strategy and the old strategy for action a_t. $\hat{A}_t$ represents the advantage function. ε denotes the clipping threshold. During the policy update process, the study uses Generalized Advantage Estimation (GAE) to approximate the advantage function. This balances bias and variance, and uses a decay coefficient of λ=0.95. This enhances the stability and sample efficiency of policy gradient estimation. Monte Carlo returns are used as a control for validation, showing consistent convergence trends in pre-experiments. The shear threshold parameter ϵ is set to 0.2 to limit the update amplitude between old and new policies, preventing policy oscillations and ensuring training stability. To address the disparity in multi-objective reward scales, the study applies linear normalization to the economic returns and ecological benefits sub-rewards. Then it combines them using the weighted coefficients from Eq. (8). This prevents any single objective from dominating during training. Thus, it achieves balanced optimization of multi-objective rewards on the same scale. This mechanism stabilizes policy updates while preserving exploration under market and ecological constraints, with the multi-objective reward function defined in Eq. (7).

$$R_t = \lambda_1 \frac{f_{eco}^* - f_{eco}(t)}{f_{eco}^*} + \lambda_2 \frac{f_{econ}(t) - f_{econ}^*}{f_{econ}^*} \tag{7}$$

In Eq. (7), $f_{eco}(t)$ and $f_{econ}(t)$ denote the ecological benefits and economic gains of step t, respectively. f_{eco}^* and f_{econ}^* both represent the reference optimal values obtained in the MOGWO-NSGA-II phase. λ_1 and λ_2 denote the weighting coefficients for ecological and economic objectives, respectively. Based on this, the overall framework of MOGWO-NSGA-PPO is illustrated in Fig.3.

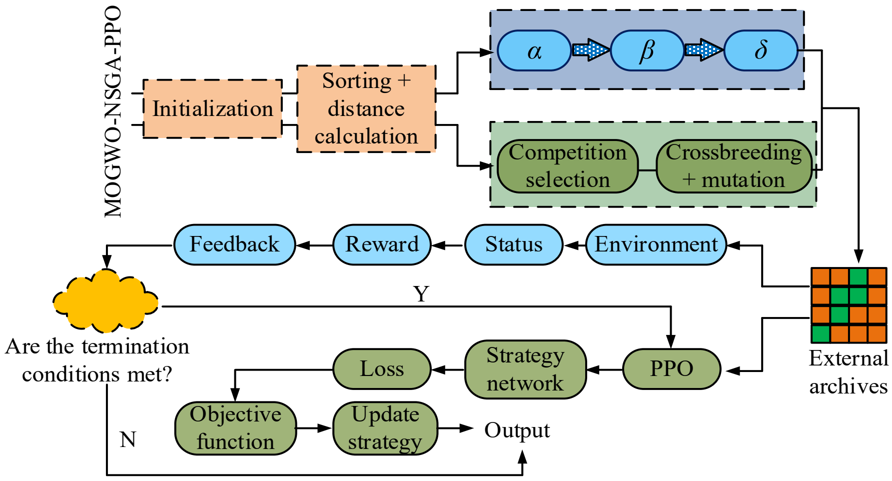

Fig. 3. The overall framework of the MOGWO-NSGA-PPO

As shown in Fig. 3, the MOGWO-NSGA-PPO framework follows a global search–elite retention–dynamic decision paradigm, in which MOGWO performs population exploration, NSGA-II maintains Pareto diversity, and PPO enables adaptive policy updates in response to real-time market and climate feedback, ultimately yielding the optimal planting strategy.

2.2. Multi-Objective Model Construction for Crop Planting Planning and Ecological Benefits

Following the algorithm design, a multi-objective optimization model is constructed using 2024 national crop production and market data, incorporating yields, costs, prices, and ecological indicators to quantify economic efficiency and environmental impacts across major crops (Table 1) (Bhosle and Musande, 2023; Chouhan et al., 2024; Basaligheh and Dhabliya, 2023).

Table 1 reveals clear differences in economic efficiency and ecological benefits among crops: corn shows the highest profitability and scale efficiency, rice and sorghum provide stable returns with ecological advantages, soybeans and rapeseed exhibit low input costs and strong eco-friendliness, while wheat remains intermediate. Based on these characteristics, an indicator system covering output efficiency, input costs, and ecological friendliness is constructed and weighted using the analytic hierarchy process. The weighting results are shown in Table 2.

As shown in Table 2, the weighting scheme prioritizes economic returns, cost control, and ecological benefits, with emission reduction emphasized as the key ecological objective, forming the basis for a four-objective optimization model, where economic benefit maximization is defined in Eq. (8).

$$f_1 = max \sum_{i=1}^{z} p_i y_i x_i - \sum_{i=1}^{z} c_i x_i \tag{8}$$

In Eq. (8), p_i denotes the unit selling price of crop type i. y_i represents the yield per unit area. x_i indicates the planting area of crop type i. c_i signifies the comprehensive cost per unit area. z represents the crop type. Input cost minimization is expressed as shown in Eq. (9).

$$f_2 = min \sum_{i=1}^{n} (k_{i1}s_i + k_{i2}s_i + k_{i3}s_i + k_{i4}s_i) x_i \tag{9}$$

In Eq. (9), s_i, f_i, m_i, and h_i represent the unit area costs for seeds, fertilizers, machinery operations, and labor/management for the i crop type, respectively. $k_{i1} - k_{i4}$ denotes their respective relative coefficients in the total cost. The maximization of ecological emission-reduction potential is given by Eq. (10).

Table 1. The main input-output benefits of crops on the farm

Category	Item	Rice	Wheat	Maize	Soybean	Rapeseed	Sorghum
Output	Yield (kg/hm^2)	9300	6400	10300	3200	2850	4600
	Total production value (RMB/hm^2)	20800	15050	23300	9000	7800	12800
Input	Seed cost (RMB/hm^2)	680	540	600	480	460	520
	Fertilizer cost (RMB/hm^2)	10850	7400	8700	4400	4200	5800
	Pesticide cost (RMB/hm^2)	1260	970	1180	570	490	720
	Machinery operation cost (RMB/hm^2)	2500	1950	2700	1150	980	1550
	Labor & management cost (RMB/hm^2)	2900	2200	2650	1250	1100	1750
Benefit	Net Profit (RMB/hm^2)	3200	2100	4700	1650	1380	2550
	Input-output ratio	1.18	1.14	1.23	1.08	1.11	1.16
	Carbon reduction potential (kg CO_2/hm^2)	820	760	880	640	600	720

Table 2. Crop planting planning, ecological benefit evaluation index system, and weight

Criterion layer	Weight	Indicator	Weight
Output benefit	0.40	Yield (kg/hm^2)	0.25
		Total production value (RMB/hm^2)	0.40
		Net profit (RMB/hm^2)	0.35
Input cost	0.35	Fertilizer cost (RMB/hm^2)	0.30
		Labor & management cost (RMB/hm^2)	0.25
		Machinery operation cost (RMB/hm^2)	0.20
		Pesticide cost (RMB/hm^2)	0.25
Ecological friendliness	0.25	Input-output ratio	0.35
		Carbon reduction potential (kg CO_2/hm^2)	0.40
		Seed cost (RMB/hm^2)	0.25

$$f_3 = max \sum_{i=1}^{n} e_i x_i \tag{10}$$

In Eq. (10), e_i represents the ecological emission reduction potential of crop type i. Input-output efficiency maximization is shown in Eq. (11).

$$f_4 = max \frac{\sum_{i=1}^{n} p_i y_i x_i}{\sum_{i=1}^{n} c_i x_i} \tag{11}$$

In Eq. (11), the numerator represents the total output value of all crops, while the denominator denotes the total input cost of all crops. The final multi-objective weighted comprehensive optimization is shown in Eq. (12).

$$F = max[w_1 f_1 - w_2 f_2 + w_3 f_3 + w_4 f_4] \tag{12}$$

In Eq. (12), w_1, w_2, w_3, and w_3 represent the composite weights for the four sub-objectives of economic benefits, cost constraints, ecological emission reduction, and efficiency enhancement, respectively, with $w_1 + w_2 + w_3 + w_4 = 1$. Based on this, a multi-objective model for the benefits of digital economy crop cultivation is constructed. Based on this model, a dedicated MOGWO-NSGA-PPO solution framework is further designed, as illustrated in Fig. 4.

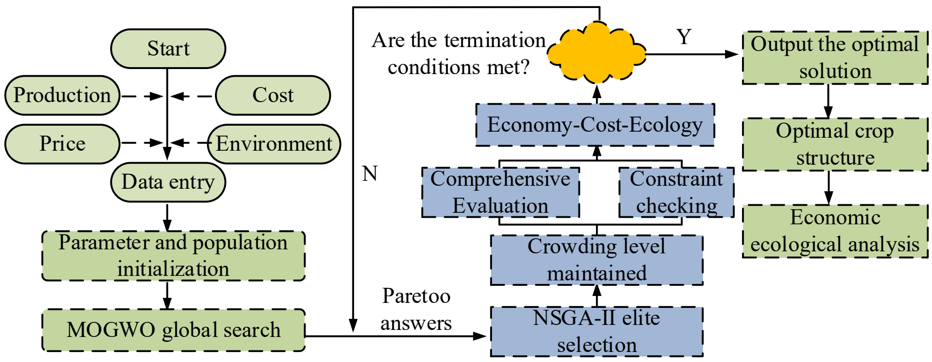

Fig. 4. The solution route based on MOGWO-NSGA-PPO

Fig. 4 shows the overall solution pipeline, in which digital economic and environmental data are standardized and optimized through an MOGWO-based global search, an NSGA-II–based Pareto refinement, and a PPO-driven dynamic adjustment under market and climate feedback, iteratively producing the optimal planting structure with corresponding economic and ecological evaluations.

3. Results

A MOGWO–NSGA-II–PPO–based multi-objective model is evaluated through parameter tuning, ablation studies, and benchmark tests to verify its convergence, stability, and optimization performance.

3.1. Algorithm Performance Testing

The experimental platform utilizes an Intel Xeon Gold 6248 CPU (2.5 GHz, 20 cores) paired with an NVIDIA RTX 3090 GPU (24 GB of VRAM), with 256 GB of DDR4 main memory. It runs on Ubuntu 20.04 LTS, with Python 3.9 serving as the primary programming and computational environment, integrated with PyTorch 1.12 and CUDA 11.3. The study first conducts selection tests across four categories of hyperparameters that affect the algorithm to determine the optimal model configuration. The test results are shown in Fig. 5.

Figures 5(a) to 5(d) present the selection test results for the contraction factor $\vartheta(t)$, the real number encoding simulation parameter X_k' for genetic recombination, the ecological objective weighting coefficient λ_1, and the economic objective weighting coefficient λ_2, respectively. As shown in Fig. 5(a), a contraction factor of 0.6 yields the fastest convergence and lowest final loss, indicating a balanced trade-off between global exploration and local exploitation. In Fig. 5(b), a genetic encoding parameter of 0.5 achieves superior convergence speed and stability, supporting effective solution diversity. Fig. 5(c) shows that an ecological weight of 0.75 leads to smoother loss reduction and higher final accuracy, highlighting the benefit of strengthening ecological constraints. Fig. 5(d) indicates that an economic weight of 0.65 provides optimal overall performance by preserving profitability while avoiding premature convergence. Collectively, the parameter combination (0.6, 0.5, 0.75, 0.65) offers the best balance between convergence efficiency, solution quality, and stability, and is therefore adopted in subsequent experiments. The study further conducts ablation tests on the MOGWO-NSGA-PPO algorithm. Results are shown in Fig. 6.

Fig. 6 reports ablation results on the FAOSTAT-CPS and CMFD-Agr datasets. While all methods show decreasing Spacing with iterations, MOGWO-NSGA-PPO converges fastest, stabilizing at about 0.08 on FAOSTAT-CPS and 0.07 on CMFD-Agr, representing an improvement of roughly 58% over GWO and outperforming MOGWO and MOGWO-NSGA. These results confirm its superior convergence speed, Pareto uniformity, and cross-dataset stability. Further comparisons with NSGA-III, MOEA/D, and SPEA2 on benchmark functions are presented in Fig. 7.

Figures 7(a) to 7(l) compare the Pareto frontiers of NSGA-III, MOEA/D, SPEA2, and the proposed MOGWO-NSGA-PPO on the DTLZ benchmark functions. As shown in Fig. 7, the proposed MOGWO-NSGA-PPO achieves the best Pareto frontier coverage on DTLZ1, DTLZ2, and DTLZ3. For DTLZ1, it attains a coverage exceeding 95%, outperforming NSGA-III (88%), MOEA/D (83%), and SPEA2 (80%). Similar advantages are observed on DTLZ2, where coverage remains above 92%, compared with about 85%, 81%, and 79% for the three benchmarks. Even for the high-dimensional, non-convex DTLZ3, MOGWO-NSGA-PPO maintains coverage above 90%, substantially higher than that of NSGA-III (82%), MOEA/D (78%), and SPEA2 (75%). These results demonstrate the proposed method's superior global convergence and its ability to approximate the Pareto frontier across increasingly complex problems.

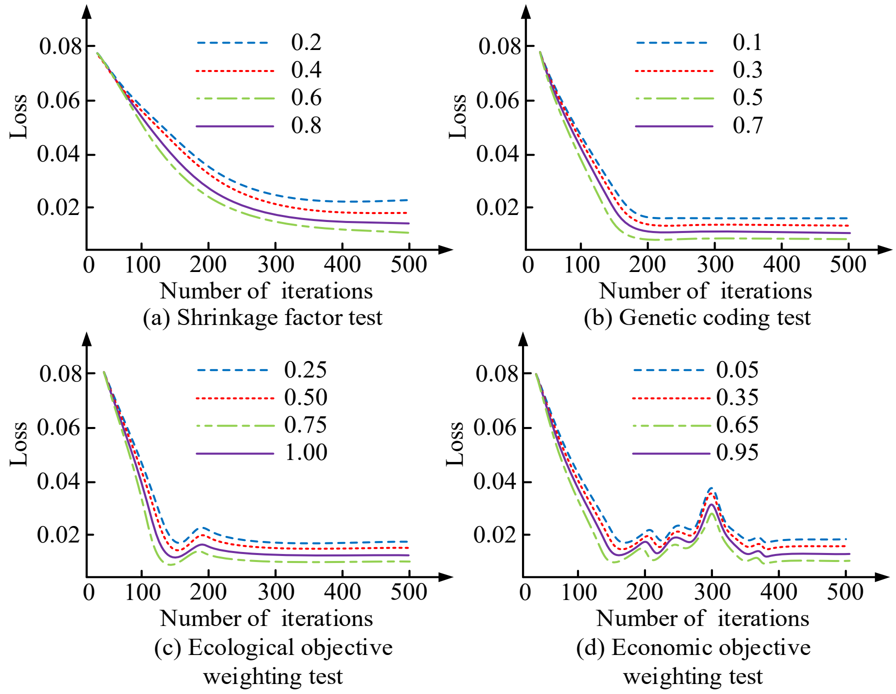

Fig. 5. Super parameter selection test results

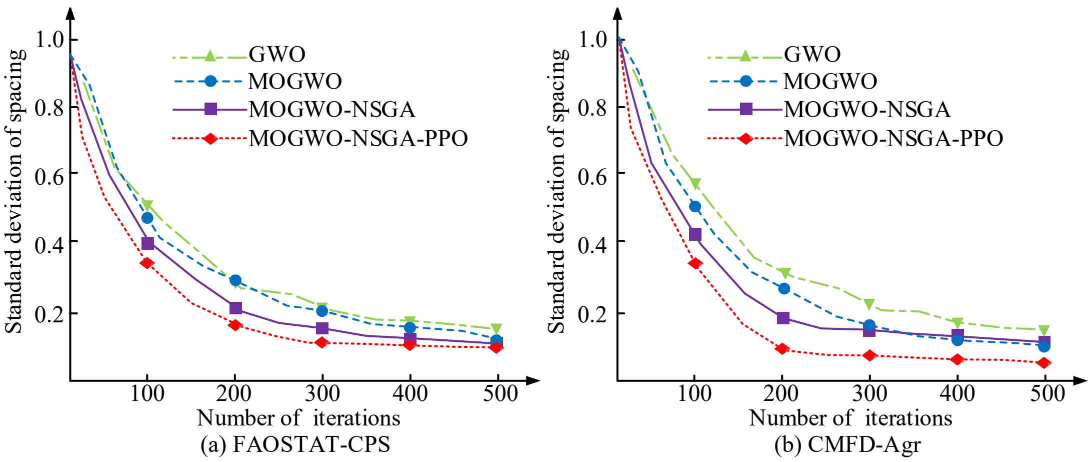

Fig. 6. Ablation test results

To further validate the stability and statistical reliability of experimental results under different random initialization conditions, the study conducts multiple runs of the main comparison algorithms with different random seeds within a unified hyperparameter grid. The mean values and 95% confidence intervals of their convergence metrics are statistically analyzed. The results are summarized in Table 3.

As shown in Table 3, the convergence performance of various algorithms varies significantly under uniform hyperparameter search ranges and random initialization conditions. The traditional GWO achieves a final mean spacing of 0.19, with a relatively wide 95% confidence interval, indicating weak stability in the distribution of the solution set. Both MOGWO and MOGWO-NSGA demonstrate improvement after the introduction of multi-objective mechanisms, with spacing values decreasing to 0.14 and 0.11, respectively. By contrast, the proposed MOGWO-NSGA-PPO achieves an average final spacing of only 0.08 across ten independent runs. This is accompanied by the narrowest 95% confidence interval and the fewest convergence iterations. This demonstrates superior convergence consistency and distribution stability under varying random conditions, further validating the reliability advantages of its multi-layer collaborative structure in multi-objective optimization.

3.2. Simulation Testing of Multi-Objective Models for Crop Planting Planning and Ecological Benefits

To evaluate the proposed method in crop planting and ecological optimization, multi-scenario simulations are conducted using farm input–output data and the FAOSTAT-CPS and CMFD-Agr datasets. MOGWO, MOGWO-NSGA, MOGWO-NSGA-PPO, and GWO are compared under identical constraints while accounting for uncertainties in arable land area and crop proportions. The resulting planting structures and integrated economic and ecological outcomes are shown in Fig. 8.

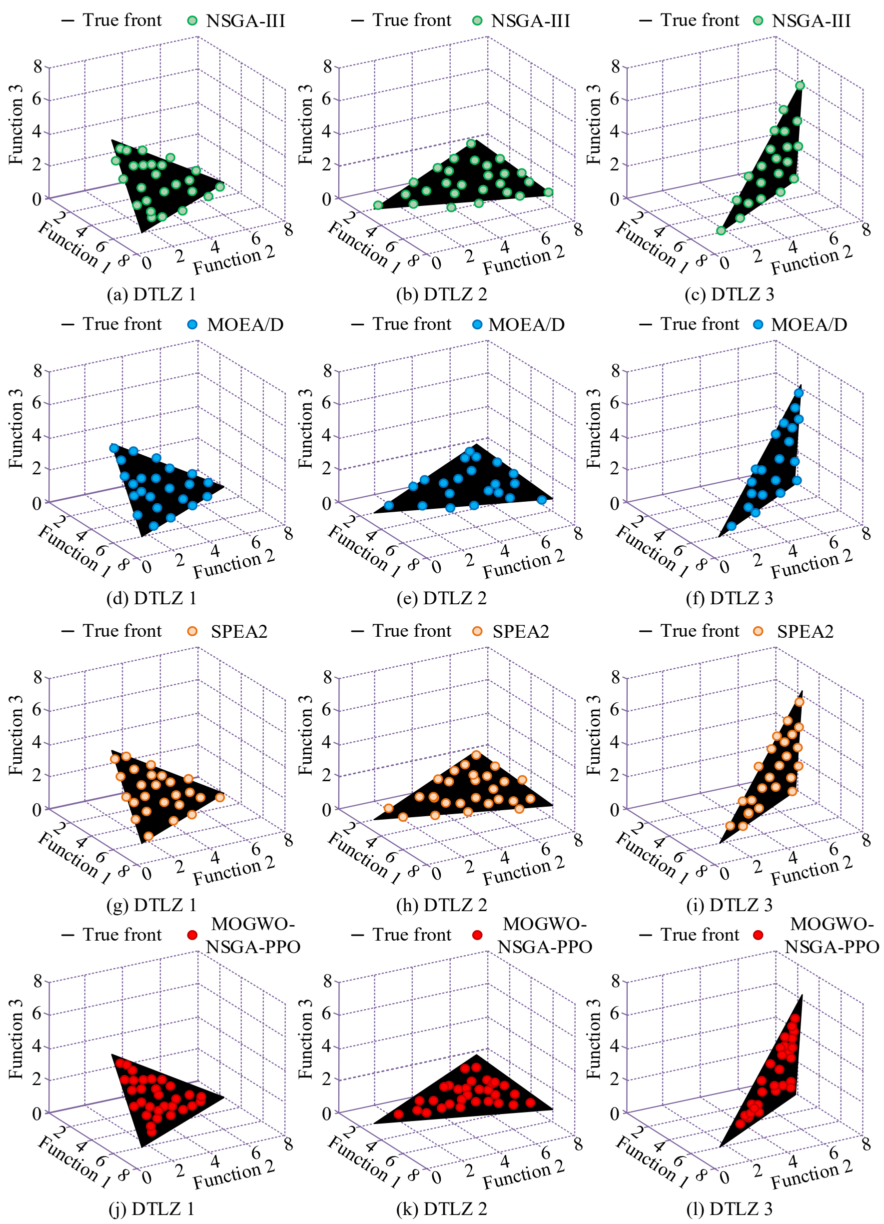

Fig. 7. Pareto frontier solution of each algorithm in DTLZ series function

Table 3. Statistical results of hyperparameter setting and convergence performance (mean ± 95% CI)

Algorithm	Hyperparameter Grid	Random Seeds	Runs	Convergence Metric (Spacing)	Mean ± 95% CI	Iterations to Convergence
GWO	a ∈ [0.2,0.8]	1–10	10	Final Spacing	0.19 ± 0.012	480±25
MOGWO	a ∈ [0.3,0.7]	1–10	10	Final Spacing	0.14 ± 0.010	420±22
MOGWO-NSGA	a ∈ [0.3,0.7], pc ∈ [0.4,0.7]	1–10	10	Final Spacing	0.11 ± 0.008	380±20
MOGWO-NSGA-PPO	a ∈ [0.3,0.7], pc ∈ [0.4,0.7], ε ∈ [0.1,0.3]	1–10	10	Final Spacing	0.08 ± 0.006	345±18

Fig. 8(a) shows that annual net income increases with cultivated area for all methods, while MOGWO-NSGA-PPO consistently achieves the highest returns, exceeding 1.5 million yuan/year at 150 ha and peaking at about 1.85 million yuan/year around 200 ha, outperforming NSGA-III, MOEA/D, and SPEA2. Fig. 8(b) indicates a unimodal relationship between net profit and arable land proportion, with MOGWO-NSGA-PPO reaching the highest peak of approximately 1.8 million yuan/year at a proportion of 0.7 and maintaining more stable returns as the proportion approaches 1.0. Overall, the proposed method demonstrates superior profitability and robustness under varying land scales and planting proportions. Continuing the comparison of total carbon emissions reductions between conventional planting and the research method across different crop allocation areas, the results are shown in Fig. 9.

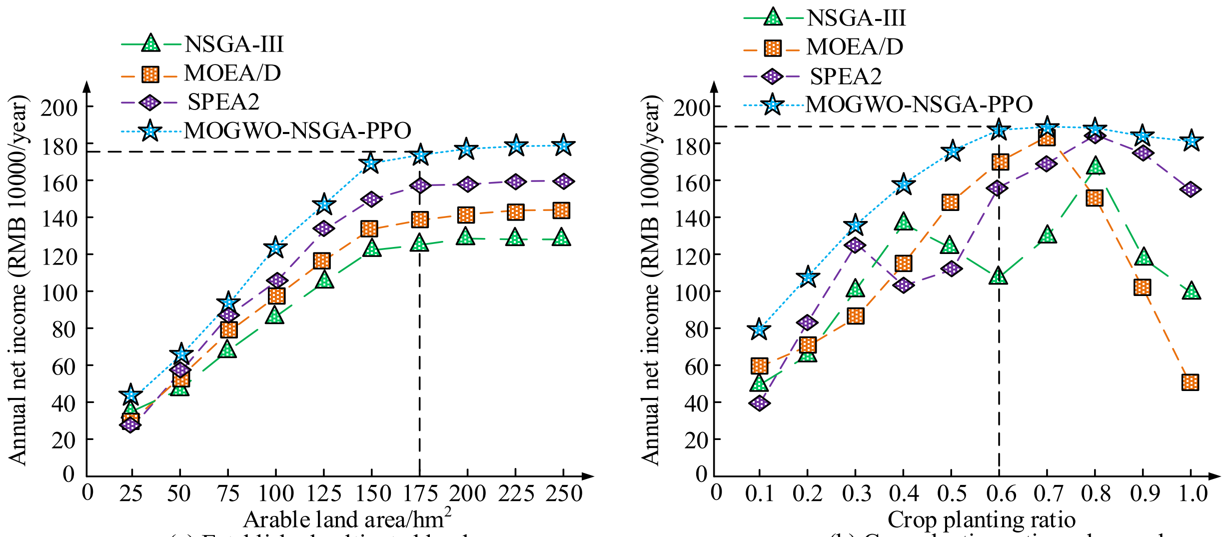

(a) Established cultivated land area and annual net income results
(b) Crop planting ratio and annual net profit results

Fig. 8. Crop planting structure and yield under different strategies

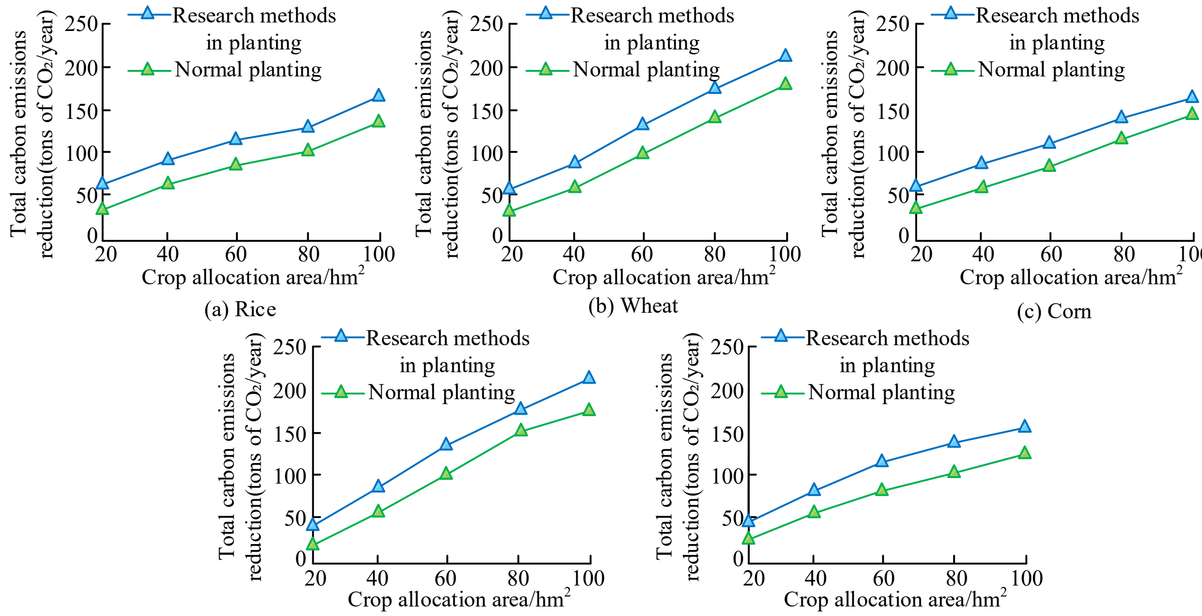

(a) Rice
(b) Wheat
(c) Corn
(d) Soybeans
(e) Rapeseed

Fig. 9. Reduction under different crop allocation areas

Figs. 9(a) to 9(e) present the total carbon emissions reductions for rice, wheat, corn, soybeans, and rapeseed under the study method and conventional farming practices, respectively. Figure 9 compares total carbon emission reductions across five crop types under different allocated areas. For all crops, the proposed method consistently achieves higher and faster-growing carbon reduction than conventional practices. As the cultivation area increases from 20 to 100 ha, carbon reduction for rice rises from 65 to 210 tons CO_2/year (25% improvement), while wheat increases from roughly 50 to 180 tons CO_2/year (22%). Corn shows the most pronounced gain, increasing from 70 to 230 tons CO_2/year (30%), followed by soybeans (40 to 160 tons CO_2/year, 28%) and rapeseed (35 to 150 tons CO_2/year, 27%). Overall, the proposed approach maintains stable emission reduction advantages across all area ranges, with particularly strong performance for corn and rice, indicating its effectiveness in enhancing carbon mitigation without compromising economic returns. The study tests the expected net benefit (RMB/ha) under 95% confidence intervals for each method in scenarios of price volatility and precipitation deviation. The results are shown in Fig. 10.

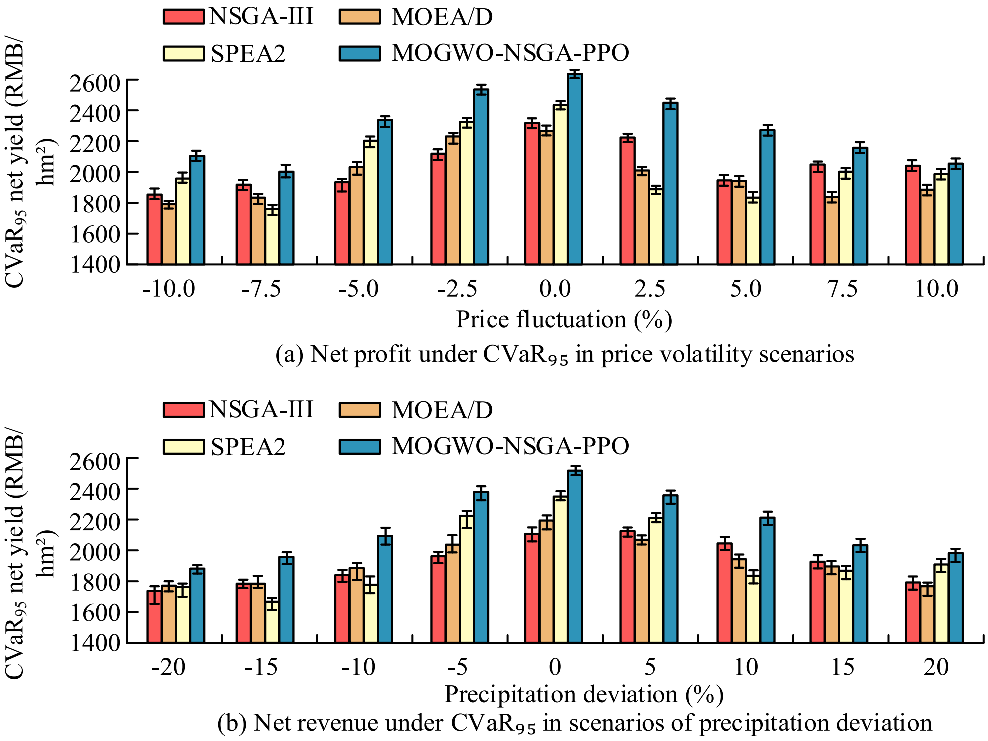

(a) Net profit under $CVaR_{95}$ in price volatility scenarios

(b) Net revenue under $CVaR_{95}$ in scenarios of precipitation deviation

Fig. 10. CVaR95 net returns under price fluctuations and precipitation deviation scenarios

Fig. 10 reports CVaR95 net returns under uncertainty in prices and precipitation. As shown in Fig. 10(a), all methods exhibit an inverted-U trend within price fluctuations of -10% to +10%, while MOGWO-NSGA-PPO consistently achieves the highest returns, peaking at about 2600 yuan/hm² near zero price fluctuation. This corresponds to improvements of approximately 24%, 30%, and 37% over NSGA-III, MOEA/D, and SPEA2, respectively. In Fig. 10(b), a similar unimodal pattern is observed under precipitation deviations from -20% to +20%, with MOGWO-NSGA-PPO reaching a maximum of about 2500 yuan/hm^2 at around +5% deviation, again clearly outperforming the benchmark methods. Overall, these results indicate that the proposed approach delivers superior robust returns and risk resilience under both market and climate uncertainties. The study further conducts a comprehensive evaluation of the four methods across three scenarios: the benchmark market, a 10% price decline, and a 15% drought. The results are presented in Table 4.

Table 4 summarizes performance under the baseline, price-decline, and drought scenarios. Under baseline conditions, the proposed method achieves a CVaR95 net return of 2590.0 yuan/hm^2, exceeding NSGA-III, MOEA/D, and SPEA2 by clear margins, while delivering the highest annual carbon reduction of 185 tons CO_2 and the shortest computation time of 4.7 s per 100 iterations. When prices decrease by 10%, the method maintains a high CVaR95 return of 2470.0 yuan/hm² and a carbon reduction of 176 tons of CO2/year, while keeping computation time below 4.8 s. Even under a 15% drought scenario, it maintains robust performance, achieving 2390.0 yuan/hm2 in CVaR95 returns, 170 tons of CO2/year in emissions reduction, and a computation time of only 4.9 s. Overall, the proposed approach consistently outperforms benchmark methods across economic, ecological, and computational dimensions, demonstrating strong robustness under market and climate uncertainties.

4. Discussion

This study addressed key limitations of traditional crop planting planning by integrating MOGWO, NSGA-II, and PPO into a digitalized multi-objective optimization framework. Experimental results showed consistent performance improvements, with Pareto frontier coverage exceeding 90% on the DTLZ benchmarks and reaching about 95% on DTLZ1, clearly outperforming NSGA-III, MOEA/D, and SPEA2. Across FAOSTAT-CPS and CMFD-Agr datasets, Spacing converged to 0.07–0.08 within approximately 350 iterations, representing a 58% improvement over GWO.

In multi-scenario simulations, CVaR95 net returns reached 2590.0, 2470.0, and 2390.0 yuan/hm² under baseline, price-decline, and drought conditions, respectively, alongside annual carbon reductions of 185, 176, and 170 tons CO_2, while computation time remained stable at 4.7 to 4.9s per 100 iterations. From a mechanistic perspective, the PPO's shear-probability-suppressed strategy suppressed oscillations under price volatility and climate perturbations. It did so by limiting the magnitude of policy updates through the objective function. This enhanced decision stability in scenarios with price floor constraints. The introduced CVaR risk metric enables policies updated to explicitly address extreme loss scenarios while optimizing expected returns, prioritizing lower-risk exposure strategies during price declines and drought conditions. Simultaneously, the advantage function estimation and shear constraint jointly regulated the exploration-utilization trade-off, preventing early-stage local optima and maintaining stable output during convergence. The model's superior CVaR performance and stable evolution trajectory across multi-scenario tests are explained by this collaborative mechanism of "constrained policy updating, risk-aware reward, and dynamic exploration regulation". These advantages arise from the complementary roles of MOGWO in global search, NSGA-II in maintaining Pareto diversity, and PPO in dynamically adapting to market and climate uncertainty. Compared with existing genetic or hybrid swarm-based approaches, the proposed framework achieves faster convergence and effective real-time adaptation. Nonetheless, reliance on structured datasets remains a limitation, and future work will explore multi-modal data integration and scenario simulation to enhance robustness under complex agricultural conditions.

Table 4. Planting, planning, and ecological benefit results under different environments

Environ ment	Indicator	NSGA-III	MOEA/D	SPEA2	Proposed method
Baseline market	CVaR95 net yield (RMB/hm^2) ↑	1780.0	2085.0	2320.0	2590.0
	Total carbon reduction (tons CO_2/year) ↑	135.0	152.0	168.0	185.0
	Computation time /100 iterations (s)↓	6.5	5.4	5.0	4.7
price decline 10 %	CVaR95 net yield (RMB/hm^2) ↑	1600.0	1950.0	2210.0	2470.0
	Total carbon reduction (tons CO_2/year) ↑	128.0	144.0	160.0	176.0
	Computation time/100 iterations (s)↓	6.6	5.5	5.1	4.8
Drought −15 %	CVaR95 net yield (RMB/hm^2) ↑	1505.0	1860.0	2125.0	2390.0
	Total carbon reduction (tons CO_2/year) ↑	120.0	138.0	154.0	170.0
	Computation time/100 iterations (s)↓	6.6	5.5	5.1	4.9

5. Conclusion

This study proposed a digital-economy-oriented multi-objective crop cultivation model integrating MOGWO, NSGA-II, and PPO. From a methodological standpoint, traditional dynamic programming struggled with dimensionality in high-dimensional state spaces. This rendered it unsuitable for multi-crop scenarios, diverse conditions, and continuous decision-making. While model predictive control offers rolling optimization advantages, its heavy reliance on system models renders it vulnerable to model bias in volatile pricing and climate-driven environments. In contrast, the proposed MOGWO-NSGA-PPO framework eliminated the need for explicit system modeling. It simultaneously achieved multi-objective optimization, risk constraints, and dynamic environmental responsiveness through a synergistic mechanism that combined swarm-intelligence-based global search with adaptive policy-gradient updates. This framework demonstrated superior scalability and robustness in complex agricultural decision-making scenarios, thereby outperforming classical programming and control methods.

While the proposed model demonstrates strong robustness to benefits and ecological synergy in multi-scenario simulations, it still has limitations. First, the model relies on structured statistical and meteorological data, such as FAOSTAT-CPS and CMFD-Agr. Its ability to adapt to unstructured, multi-source data, such as remote sensing imagery and agricultural machinery sensors, requires further validation. Secondly, the experimental scenarios are based primarily on typical regional agricultural parameters. Their applicability across different climate zones, crop structures, and policy environments must be tested using larger, cross-regional datasets. Future research could integrate multimodal data from remote sensing and the IoT, incorporate causal inference and scenario-simulation mechanisms, and validate the model's generalization capabilities through long-term, multi-regional empirical studies. This would enhance the model's applicability and the reliability of its decisions in complex agricultural ecosystems.

Funding

The research is supported by the 2025 Henan Provincial Research Project on Philosophy and Social Science Education. Research on the Path of Digital Economy Empowering Rural Revitalization in Henan Province (2025JYQS0082); 2025 Henan Province Soft Science Project. Empirical Analysis and Practical Path Research on the Impact of Digital Economy on Farmers' Income Growth in Henan Province (252400411207); 2026 Henan Province Higher Education Institutions Humanities and Social Sciences Research Funding Project: Research on the Pathways of Digital Economy Empowering High-Quality Development of Modern Service Industry in Henan Province (2026-ZZJH-200).

Institutional Review Board Statement

Not applicable.

Declaration of Artificial Intelligence (AI) Tools

The author used DeepSeek solely for language editing and readability improvement. The author reviewed and verified all content and takes full responsibility for the accuracy and integrity of the manuscript.

References

Ahila, A., Prema, V., Ayyasamy, S., and Sivasubramanian, M. (2024). An enhanced deep learning model for high-speed classification of plant diseases with bioinspired algorithm. *Journal of Supercomputing*, 80(3), 3713–3737. doi: 10.1007/s11227-023-05622-4.

Alhussan, A. A., Khafaga, D. S., Abotaleb, M., Mishra, P., and Kenawy, E. S. (2024). Global potato production forecasting based on time series analysis and advanced waterwheel plant optimization algorithm. *Potato Research,* 67(4), 1965–2000. doi: 10.1007/s11540-024-09728-x.

Bajelani, S., Shabanlou, S., Yosefvand, F., Izadbakhsh, M. A., and Rajabi, A. (2024). Optimal exploitation of water resources by using new multi-objective reptile search algorithm (MORSA). *Water Resources Management,* 38(12), 4711–4734. doi: 10.1007/s11269-024-03884-y.

Basaligheh, P., and Dhabliya, R. (2023). Precision agriculture through deep learning algorithms for accurate diagnosis and continuous monitoring of plant diseases. *Research Journal of Computer Systems Engineering,* 4(2), 31–45. doi: 10.52710/rjcse.72.

Bhosle, K. and Musande, V. (2023). Evaluation of Deep Learning CNN Model for Recognition of Devanagari Digit. *Artificial Intelligence and Applications*, 1(2), 114–118. doi: 10.47852/bonviewAIA3202441.

Bilal, A., Liu, X., Long, H., Shafiq, M., and Waqar, M. (2023). Increasing crop quality and yield with a machine learning-based crop monitoring system. *Computers, Materials & Continua*, 76(2), 2401–2426. doi: 10.32604/cmc.2023.037857.

Cai, G., Qian, J., Song, T., Zhang, Q., and Liu, B. (2023). A deep learning-based algorithm for crop disease identification positioning using computer vision. *International Journal of Computer Science and Information Technology,* 1(1), 85–92. doi: 10.62051/ijcsit.v1n1.12.

Chikkasiddaiah, C., Govindaswamy, P., and Srikantaswamy, M. (2023). An efficient hydro-crop growth prediction system for nutrient analysis using machine learning algorithm. *International Journal of Electrical and Computer Engineering,* 13(6), 6681–6690. doi: 10.11591/ijece.v13i6.pp6681-6690.

Choudhury, S. S., Pandharbale, P. B., Mohanty, S. N., and Jagdev, A. K. (2024). An acquisition based optimised crop recommendation system with machine learning algorithm. *EAI Endorsed Transactions on Scalable Information Systems*, 11(1), 411–419. doi: 10.4108/eetsis.4003.

Chouhan, S. S., Singh, U. P., Sharma, U., and Jain, S. (2024). Classification of different plant species using deep learning and machine learning algorithms. *Wireless Personal Communications*, 136(4), 2275–2298. doi: 10.1007/s11277-024-11374-y.

Demilie, W. B. (2024). Plant disease detection and classification techniques: a comparative study of the performances. *Journal of Big Data,* 11(1), 5–13. doi: 10.1186/s40537-023-00863-9.

Ghosh, S., Singh, A., and Kumar, S. (2023). BBBC-U-Net: optimizing U-Net for automated plant phenotyping using big bang big crunch global optimization algorithm. *International Journal of Information Technology,* 15(8), 4375–4387. doi: 10.1007/s41870-023-01472-8.

Guo, P., Diao, Z., Zhao, C., Li, J., Zhang, R., Yang, R., Ma, S., He, Z., Zhao, S., and Zhang, B. (2024). Navigation line extraction algorithm for corn spraying robot based on YOLOv8s-CornNet. *Journal of Field Robotics*, 41(6), 1887–1899. doi: 10.1002/rob.22360.

Heimstädt, C. (2023). Making plant pathology algorithmically recognizable. *Agriculture and Human Values,* 40(3), 865–878. doi: 10.1007/s10460-023-10419-5.

Hussien, A. G., Bouaouda, A., Alzaqebah, A., Kumar, S., Hu, G., and Jia, H. (2024). An in-depth survey of the artificial gorilla troops optimizer: outcomes, variations, and applications. *Artificial Intelligence Review,* 57(9), 246–249. doi: 10.1007/s10462-024-10838-8.

Liang, K., Lei, J., and Wu, F. (2024). Analysis of optimal planting scheme based on the North China region. *Journal of Physics: Conference Series,* 2898(1), 12004–12009. doi: 10.1088/1742-6596/2898/1/012004.

Liu, S. (2023). Planting system design and agricultural machinery configuration method for international large-scale agricultural engineering project. *Agricultural Engineering,* 13(5), 14–16. doi: 10.19998/j.cnki.2095-1795.2023.05.003.

Mahmoodabadi, M., Abedi, S., and Shakib, M. D. (2024). Optimization of logistics and industrial wastewater treatment system using grey wolf optimization algorithm. *Management Strategies in Engineering Sciences Journal,* 6(5), 69–77. doi: 10.61838/msesj.6.5.9.

Michels, V., Chou, C., Weigand, M., Wu, Y., and Kemna, A. (2024). Quantitative phenotyping of crop roots with spectral electrical impedance tomography: a rhizotron study with optimized measurement design. *Plant Methods,* 20(1), 118–121. doi: 10.1186/s13007-024-01247-7.

Pitakaso, R., Sethanan, K., Tan, K. H., and Kumar, A. (2024). A decision support system based on an artificial multiple intelligence system for vegetable crop land allocation problem. *Annals of Operations Research,* 342(1), 621–656. doi: 10.1007/s10479-023-05398-z.

Qiu, B. (2024). Optimization method of college students' entrepreneurial path based on improved multi-objective gray wolf algorithm. *Journal of Cases on Information Technology,* 26(1), 1–20. doi: 10.4018/JCIT.349738.

Rahman, F., Khan, M. A. R., and Alam, M. (2025). Hybrid PSO-GA optimization for enhancing decision tree performance in soil classification and crop cultivation prediction. *Evolutionary Intelligence,* 18(1), 30–39. doi: 10.1007/s12065-024-01015-5.

Sankareshwaran, S. P., Jayaraman, G., and Muthukumar, P. (2023). Optimizing rice plant disease detection with crossover boosted artificial hummingbird algorithm based AX-RetinaNet. *Environmental Monitoring and Assessment,* 195(9), 1070–1073. doi: 10.1007/s10661-023-11612-z.

Sarkar, S., Ganapathysubramanian, B., Singh, A., Krishnamurthy, A., Merchant, N., and Singh, A. K. (2024). Cyber-agricultural systems for crop breeding and sustainable production. *Trends in Plant Science,* 29(2), 130–149. doi: 10.1016/j.tplants.2023.08.001.

Sheikh, M., Iqra, F., Ambreen, H., Pravin, K. A., Ikra, M., and Chung, Y. S. (2024). Integrating artificial intelligence and high-throughput phenotyping for crop improvement. *Journal of Integrative Agriculture,* 23(6), 1787–1802. doi: 10.1016/j.jia.2023.10.019.

Singh, G., Sharma, S., and Singh, P. (2025). Comparative analysis of global color constancy algorithms for apple disease detection. *Applied Fruit Science,* 67(5), 314–319. doi: 10.1007/s10341-025-01541-1.

Torabi, A., Yosefvand, F., Shabanlou, S., Rajai, A., and Yaghoubi, B. (2024). Optimization of integrated operation of surface and groundwater resources using multi-objective grey wolf optimizer (MOGWO) algorithm. *Water Resources Management,* 38(6), 2079–2099. doi: 10.1007/s11269-024-03744-9.

Wang, H.,
and Zhou, B. (2025). A leader-wingman-inspired cooperative-competitive optimization algorithm for sustainable part collection routing problem. *Journal of Industrial and Management Optimization,* 21(9), 5772–5807. doi: 10.3934/jimo.2025113.

Yadav, S., Dillon, S., McNeil, M., Dinglasan, E., Mago, R., Dodds, P., Hickey, P., and Hayes, B. J. (2025). Optimising parent selection in plant breeding: comparing metaheuristic algorithms for genotype building. *Theoretical and Applied Genetics,* 138(9), 1 – 20. doi: 10.1007/s00122-025-05028-1.

Yang, F., Du, Y., Wen, C., Li, Z., Mao, E. R., and Zhu, Z. X. (2024). Optimization design of the hydro-pneumatic suspension system for high clearance self-propelled sprayer using improved MOPSO algorithm. *International Journal of Agricultural and Biological Engineering*, 17(2), 109–122. doi: 10.25165/j.ijabe.20241702.7813.

Zhang, T., Cai, Y., Zhuang, P., and Li, J. (2024). Remotely sensed crop disease monitoring by machine learning algorithms: A review. *Unmanned Systems,* 12(1), 161–171. doi: 10.1142/S2301385024500237.

Xiaohong Wang earned her Bachelor’s Degree in Economics from Jilin University from 1999 to 2003, her Master’s Degree in Political Economy from Wuhan University from 2008 to 2010, and her Doctor’s Degree in Business Administration from Stamford International University between 2020 and 2025. She holds the academic title of Associate Professor and serves as the Deputy Director of the Center for Contemporary Marxist Economics Research at Zhengzhou Technology and Business University. Her research interests include digital economy and rural economy.